Oct 26th, 12:00 AM

Buckling Behavior of Cold-formed Scaffolding Tubes

A. Hubner

H. Saal

Eighteenth International Specialty Conference on Cold-Formed Steel Structures
Orlando, Florida, U.S.A, October 26 & 27, 2006

Buckling behavior of cold-formed scaffolding tubes

Hübner, A.[1] and Saal, H.[2]

Abstract

Hollow section profiles in different variations are increasingly used in modern structures due to architectural and economic reasons. The buckling failure of column structures has been investigated thoroughly over the past century. The currently developed European standard for designing steel structures (EN 1993-1-1 [1]) considers different buckling classes for assessing compressive members. The classification for hollow sections is based on experiments involving large tubes. Cold-formed scaffolding tubes are by far smaller regarding their dimensions. This research project on the buckling behavior of cold-formed scaffolding tubes investigates whether current European design rules are justified for these dimensions. Several experiments were performed and compared with numerical approaches. Additionally, comparisons with existing design codes are performed. The results of this investigations show that for scaffolding tubes the modification of [1] in buckling design is very conservative and suggest the application of the former classification.

1. Introduction

The currently developed European standard for designing steel structures (EN 1993-1-1 [1]) considers different buckling curves for cold-formed and hot-finished hollow sections. Following the classification

[1] research assistant, Lehrstuhl für Stahl- und Leichtmetallbau, Universität Karlsruhe (TH), D-76128 Karlsruhe, Germany
[2] full professor, idem.

in Eurocode 3 [1] scaffolding tubes, which are cold-formed members, need to be assessed according to buckling curve *c* instead of buckling curve *b* as before, leading to a reduction of the carrying capacity of about 10 %. Since scaffolding columns are often used to full capacity (utilization factor of 1.0) in designs, this rule may be the knock-out criterion for some scaffolding systems. The new assessment rules are based on experiments (cfr. [2]) using hollow sections with diameters of about 200 mm. These are not representative dimensions for scaffolding tubes.
The paper describes column buckling tests on scaffolding tubes of typical dimensions. Additionally, finite element analyses were performed simulating the buckling failure of the columns. The experimental and numerical results were used to interpret the buckling phenomena of the scaffolding tubes. Subsequently, the findings were evaluated with regard to the design rules given in Eurocode 3 [1].A partial safety coefficient γ_m for the material side of 1.0 is assumed throughout this paper. The safety $\gamma_{sf,a}$ and $\gamma_{sf,b}$ values in the following indicate the safety of the experimental results with regard to the characteristic values used in the design. The prescribed partial safety coefficient $\gamma_m = 1.1$ thus applies additionally to these safety values.

2. Description of the cold-formed scaffolding tubes

For the investigation of the buckling behavior standard scaffolding tubes were chosen, which are commonly used as columns in constructions. The tubes are cold-formed and longitudinal welded tubes with a nominal cross-section Ø 48.3 mm x 3.2 mm made of standard structural steel S235JR ($f_y = 240$ N/mm^2). The length of the investigated tubes was 1.50 m (medium slenderness). For the experiments non-galvanized scaffolding tubes were used.

3. Experiments and results

The length of the tubes was re-measured and confirmed as 1.50 m for all tubes. The tube diameter and the wall thickness of the tube was measured for all tubes at several positions using a micrometer and a slide gauge. The results were evaluated statistically. The geometry fits

the tolerance requirements according to the technical delivery requirements EN 10219-2 [3]. Additionally, the geometrical bow imperfection (pass) of the tubes was measured. The measurement was performed by mounting the tube in a lathe and determining the pass by rotating the tube and referring it to a base line constructed from both ends of the tube (center of the cross-section). The results in Table 1 show that the initial bow imperfection was much less than the limit in Eurocode EN 1993-1-1 [1], which is $l/250$ = 6,0 mm for buckling curve *b* and $l/200$ = 7,5 mm for buckling curve *c*.

Table 1: Measurement of the initial bow imperfection u_{meas}

tube	1	2	3	4	5
pass [mm]	0.30	0.48	0.52	1.97	0.33

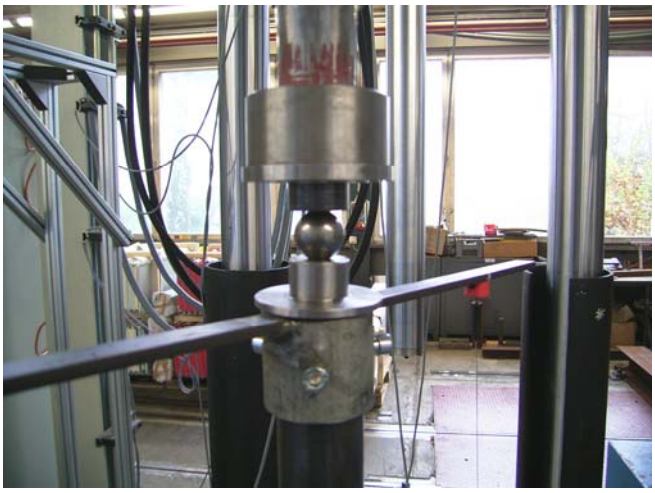

Figure 1: Top support

For obtaining the buckling load and for the evaluation of the buckling curves buckling tests were performed. The tubes were installed vertically and positioned by hinges at both ends. A pin connection was

accomplished by introducing tempered steel spheres Ø 30 mm (Figures 1 and 2).
The load introduction between sphere and tube was achieved by specially manufactured, conically shaped adapters extending into the tube. The purpose of the adapters is to center the tube and to absorb possible edge imperfections. Due to the pinned connections and the load introducing device all specimens had a buckling length of s_k = 1580 mm.

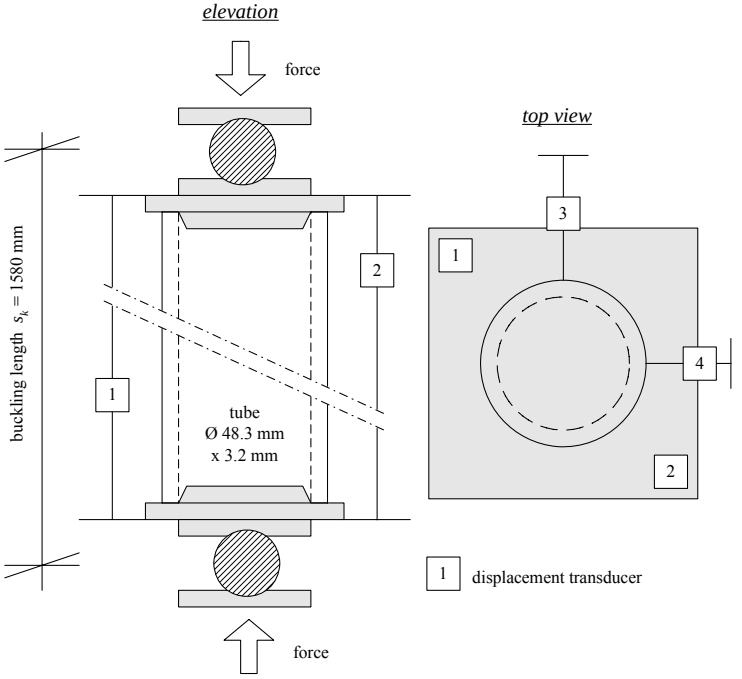

Figure 2: Sketch of test set-up

The deflection was measured continuously at midspan. Two horizontal displacement transducers were offset by 90° (transducer 3 and 4). Further, the relative shortening of the tubes was measured at opposite positions (transducer 1 and 2). Simultaneously, the induced force was recorded by the measuring system. The test set-up and the positions of

the displacement transducers are depicted in Figure 2. The results of the experiments are summarized in Table 2. With the tube at maximum load in Figure 3, the bent of the tube can be clearly seen.

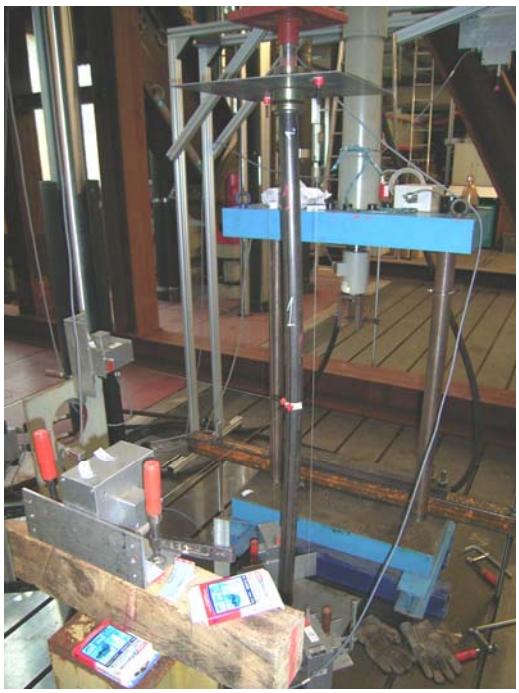

Figure 3: Picture of test set-up; maximum load

Table 2: Results from the experiments; buckling load P_u

tube	1	2	3	4	5	standard deviation s	average $P_{u,av}$
P_u [kN]	94.4	98.7	77.4	87.3	75.3	10.3 kN	86.6 kN

3 Evaluation of the test results

For the assessment according to Eurocode 3 [1] the influence of the bow imperfection is estimated. The aim of the considerations is to compare buckling loads based on the experimental results and the measured initial geometrical bow imperfections with buckling loads derived from design codes. The approach uses the buckling check for simple bending with axial force according to the German code for constructional steel DIN 18800-2 [4]. The buckling check is identical to the check in Eurocode 3 [1]. For the simply axially loaded column (N_0) the limit case for the buckling check can be written as:

$$\frac{N_0}{\kappa_0 \cdot N_{pl}} = 1 \qquad \text{or} \qquad N_0 = \kappa_0 \cdot N_{pl}$$

with the reduction factor κ_0 and the plastic resistance N_{pl} to normal forces. The buckling check for simple bending with axial force in DIN 18800-2 [4] can be written for a purely axially loaded column (N_1) with an initial geometric bow imperfection with the pass Δu as:

$$\frac{N_1}{\kappa_1 \cdot N_{pl}} + \frac{N_1 \cdot \Delta u}{M_{pl}} + \Delta n = 1$$

with the plastic resistance to bending M_{pl} and the correction factor Δn. Assuming $\kappa_0 = \kappa_1$ the two previous equations can be combined and redrafted for N_1:

$$N_1 = \frac{(1 - \Delta n) \cdot N_0}{1 + \dfrac{\Delta u \cdot N_0}{M_{pl}}}$$

Since the correction factor Δn is a function of N_1 and vice versa, the equations need to be solved iteratively.

$$\Delta n = \frac{N_1}{\kappa_1 \cdot N_{pl}} \left(1 - \frac{N_1}{\kappa_1 \cdot N_{pl}} \right) \kappa^2 \overline{\lambda}_k^2 \qquad \text{with} \quad \Delta n \le 0.1$$

The equivalent slenderness $\overline{\lambda}_k$ is a function of the corresponding buckling curve. Using the last two equations the influence of the initial bow imperfections which have to be imposed according to DIN 18800-2 [4] can be compared with the calculated values (Table 3). The buckling

loads for the corresponding more unfavorable buckling curve, i.e. *b* for *a*, and *c* for *b*, are calculated for comparison using the derived equations. Based on the buckling load N_a for buckling curve *a* and the difference between the passes ($\Delta u = l \cdot [1/250\text{-}1/300]$) a derived buckling load $N_{b,deriv}$ can be determined for buckling curve *b*. The procedure for buckling curve *c* is accordingly. Table 3 summarizes the results.

Table 3: Comparison of buckling loads

	N according to DIN 18800-2 [4]		
	N_a	N_b	N_c
buckling load [kN]	67.6	60.6	54.8
pass Δu	$l/300$	$l/250$	$l/200$
	5.27 mm	6.32 mm	7.90 mm
	N from equation for N_1		
	$N_{a,deriv}$	$N_{b,deriv}$	$N_{c,deriv}$
buckling load [kN]	-	62.8	55.6

The two sets of buckling loads in Table 3 are close to each other. The derived buckling loads N_{deriv} are about 1 % to 3.5 % smaller than the buckling loads *N* according to [4]. In the next step the test results (P_u) are compared to the buckling loads (P_{EC}) according to EN 1993-1-1 [1] or alternatively DIN 18800-2 [4].

The calculation of the buckling loads $P_{EC,check}$ is performed for the buckling check assumptions, i.e. the geometry is based on nominal values and the material properties are based on the yield stress of the parent material (S235JR). Further buckling loads $P_{EC,test}$ based on measured values (average measured geometry and yield stress from tensile tests) are calculated for the investigated specimens. The results can be found in Table 4.

The results from the experiments (P_u) have to be adjusted since the measured geometric bow imperfections are significantly smaller than the postulated values. Emanating from the good correlations found for the derived buckling loads (Table 3), the results are adjusted applying the measured imperfections u_{meas} and the following equation:

$$P_{u,red} = \frac{(1-\Delta n)\cdot P_u}{1+\frac{u_{meas}\cdot P_u}{M_{pl,act}}}$$

The plastic resistance to bending $M_{pl,act}$ and the factor Δn are calculated using the measured values (geometry and yield stress). The reduced buckling load $P_{u,red}$ can be found in Table 4.

Table 4: Buckling loads according to DIN 18800-2 [4] or EN 1993-1-1 [1] and test results

No.	P_u [kN]	$P_{EC,check}$ [kN] curve			$P_{EC,test}$ [kN] curve			$P_{u,red}$ [kN]	$\gamma_{sf,a}$ [-]	$\gamma_{sf,b}$ [-]
		a	*b*	*c*	*a*	*b*	*c*			
1	94.4	67.6	60.6	54.8	71.1	64.5	58.8	91.2	1.35	1.50
2	98.7				71.1	64.6	58.9	92.6	1.37	1.53
3	77.4				71.2	64.6	58.9	75.0	1.11	1.24
4	87.3				70.3	63.8	58.2	75.6	1.12	1.25
5	75.3				71.2	64.7	59.0	73.9	1.09	1.22

The comparison reveals that the determined buckling loads ($P_{u,red}$) are greater than the values obtained for an assessment according to the design codes. The choice of buckling curve *c* results in an underestimation of the carrying capacity by 26 % to 41 % for the investigated cases ($P_{EC,check}$). A more detailed evaluation of the buckling load ($P_{EC,test}$) based on measured data leads to an underestimation of 20 % to 36 %. The experimental results reveal that for the worst case ($P_{u,red}$ = 73.9 kN) a safety $\gamma_{sf,b}$ of 73.9/60.6 = 1.22 arises in comparison to $P_{EC,check}$ for

buckling curve *b*. In Table 4 the safety values are given for buckling curve *a* ($\gamma_{sf,a}$) and *b* ($\gamma_{sf,b}$).
Although only a set of 5 buckling tests was performed and thus the statistical evaluation of the sample should not be ascribed too much importance, a brief comparison is performed. The buckling loads $P_{u,red}$ derived from the buckling tests can be evaluated statistically. Based on a normal distribution, and a confidence coefficient of 0.75 the 5 %-percentile for the 5 tests can be evaluated as $P_{u,red,5\%}$ = 63.5 kN. Calculating the safety values $\gamma_{sf,b}$ for the statistically derived value $P_{u,red,5\%}$ results in 1.05 which exists in addition to the prescribed safety coefficient γ_m.

4. Numerical Analyses

The numerical analyses were performed using the well-known and sophisticated Finite Element program ABAQUS. In the first step of the numerical investigation scaffolding tubes were modeled. The non-linear material properties implemented in the numerical model were based on tensile tests performed with coupons taken from the specimens. Up to the yield stress (370 N/mm^2) a linear elastic model was assumed (E = 210000 N/mm^2 and μ = 0.3). The hardening and the plasticity were directly implemented as measured in the tensile tests. For the modeling of the scaffolding tubes the measured average diameters and wall thickness were used. The system was modeled with pin connections at both sides.
The analyses were performed in two steps. First, a linear buckling analysis (eigenvalue prediction) was performed and the failure eigenmode extracted. The first eigenmode of the axially loaded column is a sinus wave mode like the initial bow imperfection. Then this state is used for imposing the geometrical imperfection for the subsequent analyses. In the following step a geometrical and material non-linear load-displacement analysis involving the Riks method with the bow imperfection and the pass according to the measurement was performed. The results are summarized in Table 5.
The comparison reveals large differences between the results from the numerical analyses and the experiments. These discrepancies arise due to several reasons. The imposed bow imperfections were measured

using rather simple tools, were limited to the measurement of the maximum pass and related to the assumption of an eigenform-affine shape of bow. The buckling load $P_{u,FEM}$ is very sensitive to the bow imperfections. For example, a numerical analysis for tube 5 with a bow imperfection which is 1 mm larger than the measured value results in a buckling load $P_{u,FEM}$ = 75.8 kN, i.e. about 10 % smaller than the value given in Table 5, and close to the value of P_u. Another explanation for the differences is the implemented material model. Although the used material model is chosen according to averaged tensile tests, the buckling load changes by about 5 % for a fixed yield stress and different hardening behaviors (hardening according to the tensile tests). Further, the measured geometries are based on ten measurements, each at accessible positions. No details can be given for a thickness or diameter change over the length. If e.g. a by 0.1 mm greater wall thickness is applied for tube 5 the buckling load increases by nearly 3 %. Thus, bearing the possible inaccuracies in mind and the large sensitivity of the problem the numerical analyses deliver fairly acceptable results.

Table 5: Comparison of the characteristic values for scaffolding tubes from experiment and numerical analyses

No.	P_u [kN]	$P_{u,FEM}$ [kN]	$\Delta P_u/P_u$ [%]
1	94.4	84.2	+ 10.8
2	98.7	81.8	+ 17.1
3	77.4	82.1	- 6.1
4	87.3	71.9	+ 17.6
5	75.3	83.3	- 10.6

Another effect which has not been discussed so far is the influence of residual stresses arising from the rolling and the welding process. It is well know that the presence of residual stresses may affect buckling

loads of structures significantly. Therefore, an additional test was performed in order to investigate the residual stresses in scaffolding tubes.

5. Residual stresses

In order to get an impression of the magnitude of the residual stresses in the scaffolding tubes a specimen was manufactured from a 30 cm long piece of a tested scaffolding tube. Six strain gages were applied on half of the circumference as depicted in Figure 4. The specimen was then cut into small segments step-by-step measuring the changing strains continuously. Since no measurements could be performed on the inside of the tube and the circumferential residual stresses were assumed to be negligible, it is supposed as a first rough approximation that the measured axial strains are directly related to the axial membrane strains. The evaluated residual stress distribution is depicted in Figure 5. No distinct trend can be interpreted from the readings. Still, it can be seen that large compressive stresses of more than 300 N/mm^2 evolve near the weld and opposite to it. In order to define a stress distribution in equilibrium for a first preliminary analysis, the stresses are assumed to be present over the entire thickness with the distribution depicted in Figure 5. This procedure imposes self-equilibrating membrane residual stresses without any bending residual stresses.

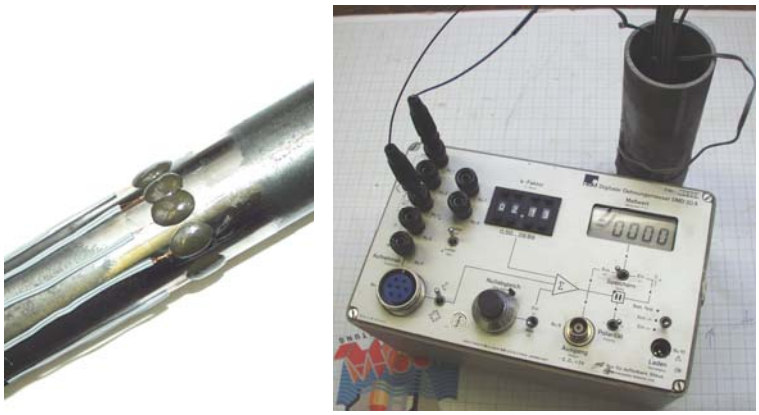

Figure 4: Applied strain gages and measuring device

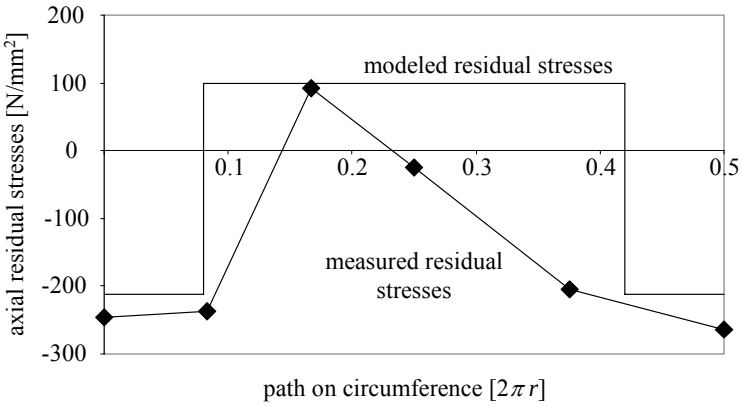

Figure 5: Modeled and measured residual stress distribution

Numerical bucking analyses were performed based on the residual stress distribution. First the residual stresses were imposed in an equilibrating step, before performing non-linear load-displacement analyses as before. Figure 6 depicts the load -displacement curves of the test results and the FE analyses for tube no. 3.

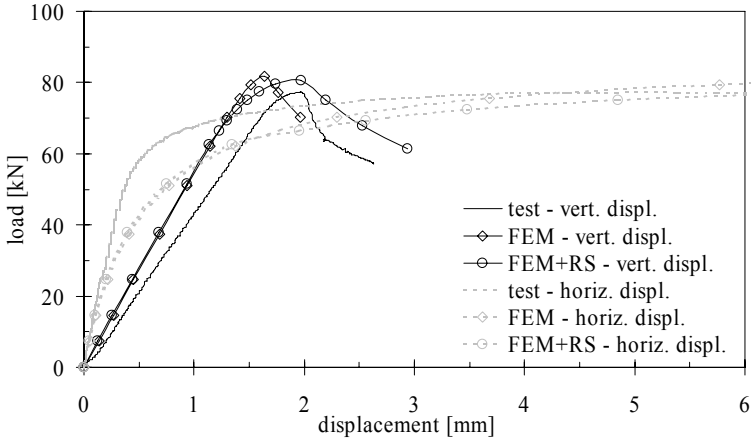

Figure 6: Load-displacement plots of test results and FE analyses for tube 3

It can be seen that the influence of the residual stresses for tube no. 3 is fairly small, as it reduces the buckling load by about 2 %. The load-deflection behavior changes slightly as the deformations increase faster after reaching the limit load. A similar behavior was found for the other tubes.
A second set of analyses imposed bending residual stresses by interpreting the measured stresses from Figure 5 as constant compressive residual stresses of 200 N/mm^2 on the outside of the shell. In order to obtain equilibrium a linear distribution over the thickness is assumed, leading to tensile residual stresses of 200 N/mm^2 on the inside of the shell. No additional membrane residual stresses are considered. For tube no. 3 a reduction of about 3 % was found for the limit load. Comparing analyses assuming a residual bending stress with the maximum stress equal to the yield stress revealed a reduction by 12 %. It can be seen that the influence on the buckling load significantly increases for larger residual stresses.
Generally, it can be seen that the influence of residual stresses for these first preliminary investigations seems to be fairly small. Nevertheless, the comparison is only based on a small number of measurements and thus can only serve as first idea for the carrying behavior.

6. Conclusions

The buckling strength of slender tubes as used in scaffoldings was investigated experimentally and numerically in order to obtain a deeper insight into the problem. Since the buckling assessment changes with the introduction of Eurocode 3 [1] for the tubes, the validity of the new rules was discussed. The aim is to evaluate the carrying behavior of scaffolding tubes concerning the buckling design with respect to design standards. The importance of the research can be clearly seen, as advanced knowledge in the field of column buckling for specific cases such as scaffolding tubes, leads to more economic and technically more elaborate constructions. The study involved a set of tests which then were evaluated and compared to numerical analyses for tubes with and without residual stresses.

Although only a small number of tests have been performed, it is assumed that the following conclusions can still be drawn from this first study:

1. For all the investigated tubes, safety values greater than 1.0 were obtained: for $\gamma_{sf,a}$ from 1.09 to 1.37, and $\gamma_{sf,b}$ from 1.22 to 1.53. Even for the 5 %-percentile of the test results a safety factor $\gamma_{sf,b} = 1.05$ was found. These safety values indicate the safety of the experimental results with regard to the characteristic values used in the design. The prescribed partial safety coefficient $\gamma_m = 1.1$ applies additionally.
2. Assessments with buckling curve *c* lead to underestimations of 25 % to 40 %.
3. Numerical studies showed deviations between tests and analyses. The differences are mainly caused by imprecisely measured imperfections.
4. The measurement of the residual stresses led to a non-uniform stress distribution with a maximum amplitude of more than 200 N/mm^2.
5. Additional preliminary numerical studies for tubes with imposed residual stresses distributions emphasized a small influence on the buckling load. For residual stresses near the yield stress the reduction becomes noticeably.

It is expected that further studies will lead to an enhanced set of buckling rules for scaffolding tubes providing a basis for more economic constructions.

7. Acknowledgements

The work presented herein was financially supported by the Förderkreis DIN/CEN-Normung (Gerüstbauhandwerk). We are grateful for their support and cooperation.

8. References

[1] EN 1993-1-1:2005-05, Eurocode 3: Design of steel structures – Part 1-1: General rules and rules for buildings.

[2] Grotman, D., Krampen, J., Sedlacek, G., Tragverhalten von Stahlprofilstützen, Stahlbau, v70, n12, pp.988-990, 2001.

[3] EN 10219-2: 2003-04, Kaltgefertigte geschweißte Hohlprofile für den Stahlbau aus unlegierten Baustählen und aus Feinkronstählen, Teil 2: Grenzabmaße, Maße und statische Werte.

[4] DIN 18800-2:1990-11, Stahlbauten, Teil 2: Stabilitätsfälle, Knicken von Stäben und Stabwerken.